Supplemental Material can be found at:
http://dmd.aspetjournals.org/content/suppl/2012/12/31/dmd.112.048975.DC1.html

1521-009X/41/3/622–633$25.00
DRUG METABOLISM AND DISPOSITION
http://dx.doi.org/10.1124/dmd.112.048975
Drug Metab Dispos 41:622–633, March 2013
Copyright © 2013 by The American Society for Pharmacology and Experimental Therapeutics

DMD
DRUG METABOLISM AND DISPOSITION

Metabolism of Saikosaponin a in Rats: Diverse Oxidations on the Aglycone Moiety in Liver and Intestine in Addition to Hydrolysis of Glycosidic Bonds[S]

Guoqiang Liu, Yuan Tian, Geng Li, Lei Xu, Rui Song, and Zunjian Zhang

Key Laboratory of Drug Quality Control and Pharmacovigilance (Gu.L., Y.T., Ge.L., L.X., R.S., Z.Z.) and State Key Laboratory of Natural Medicines (Z.Z.), China Pharmaceutical University, Nanjing, China

Received September 11, 2012; accepted December 31, 2012

ABSTRACT

The main objective of the present study was to completely characterize the metabolites of the triterpenoid saikosaponin a (SSa) in rats. To this aim, we compared the metabolites in plasma, bile, urine, and feces samples following oral and i.v. routes of administration using liquid chromatography–diode array detector coupled with hybrid ion trap–time-of-flight mass spectrometry. As a result, besides 2 known metabolites, prosaikogenin f and saikogenin f, 15 new metabolites were detected in all. It was found that SSa is metabolized mainly in phase I manner, i.e., hydration and monooxidation on the aglycone moiety and hydrolysis of the β-glucosidic bond in the liver, and sequential hydrolysis of β-glucosidic and β-fucosidic bonds followed by dehydrogenation, hydroxylation, carboxylation, and combinations of these steps on the aglycone moiety in the intestinal tract. Both the renal and biliary routes were observed for the excretion of SSa and its metabolites. Further, a clear metabolic profile in rats was proposed in detail according to the results from the in vivo animal experiment after different routes of administration. Our results update the preclinical metabolism and disposition data on SSa, which is not only helpful for the future human metabolic study of this compound but also provides basic information for better understanding of the efficacy and safety of prescriptions containing saikosaponins.

Introduction

Saikosaponins, the major bioactive ingredients of the genus *Bupleurum* with a long history of medicinal use, exert significant pharmacological activities, including antitumor (targeting various cancer cells) (Motoo and Sawabu, 1994; Ahn et al., 1998; Hsu et al., 2000; Tsai et al., 2002; Wen-Sheng, 2003; Hsu et al., 2004; Kim and Hong, 2011), chemosensitizing (Wang et al., 2010a), anti-inflammatory (Yokoyama et al., 1981; Nose et al., 1989a; Bermejo Benito et al., 1998), immunomodulatory (Kumazawa et al., 1989; Leung et al., 2005; Sun et al., 2009), hepatoprotective (Abe et al., 1980; Fan et al., 2007; Wu et al., 2008), antinephritic (Li et al., 2005; Chen et al., 2008; Hattori et al., 2008), antibacterial and antiviral (Kumazawa et al., 1990; Chiang et al., 2003; Cheng et al., 2006), estrogenic (Wang et al., 2010b), and promoting amylase secretion in rat pancreatic acini (Yu et al., 2002). On the other hand, saikosaponins have also been reported to be responsible for toxicity induced by their hemolytic action (Abe et al., 1978a, b; Nose et al., 1989b). Moreover, the poor selectivity resulting from the broad spectrum of pharmacological activity of saikosaponins puts at risk the clinical applications of prescriptions containing them, especially in combination with other drugs, with drug-drug interactions taken into consideration. In general, therapeutic application of saponins is very limited because of either the poor absorbance from the intestine when taken orally or the toxicity induced by marked hemolysis when administered by injection, especially i.v. (Segal et al., 1978). Better understanding of the efficacy and safety of saikosaponins requires the elucidation of their biologic fates in the body.

Although the pharmacokinetics of saikosaponin a, b1, b2, c, and d in rats after i.v. or oral administration has been reported (Shimizu et al., 1984; Fujiwara and Ogihara, 1986; Kida et al., 1998; Tang et al., 2007; Xu et al., 2012), there was limited knowledge about the in vivo metabolism of these compounds. Study of the metabolism of saikosaponins has mainly been focused on the artificial isomers in gastric conditions and deglycosylation metabolites by intestinal bacteria (Shimizu et al., 1985a). Japanese researchers reported that saikosaponins are unstable in the gastric juice and prone to convert into their isomeric derivatives with the allyl oxide linkage in the 13,28 position of aglycone breaking into a heteroannular or homoannular diene. Further, these saikosaponins are hydrolyzed into their corresponding prosaikogenins and saikogenins by the hydrolyzing activities of intestinal bacteria, such as *Eubacterium* sp. A-44 (Kida et al., 1997), which were also essential for the appearance of prosaikogenin a and saikogenin a in rat plasma after oral administration of saikosaponin b1 (Kida et al., 1998). Although the total recovery of excreted saikosaponin a (SSa), prosaikogenin f (PSGf), and saikogenin f (SGf) in the feces of conventional rats was >50% of the starting dose in a period over 0 to 24 hours after the oral administration of SSa (Shimizu et al., 1985a), the disposition of <50% remained unexplained. The whole metabolic profile of SSa cannot be reflected by only deglycosylation metabolites

This study was financially supported by the National Natural Science Foundation of China [Grant 30873439].
dx.doi.org/10.1124/dmd.112.048975.
[S]This article has supplemental material available at dmd.aspetjournals.org.

ABBREVIATIONS: fuc, fucose; glc, glucose; HOSSa, hydroxysaikosaponin a; LC, liquid chromatography; LC-DAD-IT-TOF-MS, liquid chromatography–diode array detector coupled with hybrid ion trap–time-of-flight mass spectrometry; MF, molecular formula; MS, mass spectrometry; m/z, mass-to-charge ratio; PSGf, prosaikogenin f; SGf, saikogenin f; SSa, saikosaponin a.

Downloaded from dmd.aspetjournals.org at Zhejiang University on May 1, 2013

DMD
DRUG METABOLISM AND DISPOSITION
aspet

such as PSGf and SGf, and so can that of the other saikosaponins. Thus we chose SSa as a representative of the saikosaponins to clarify its metabolic fate in rats using the liquid chromatography–diode array detector coupled with hybrid ion trap–time-of-flight mass spectrometry (LC-DAD-IT-TOF-MS) technique based on the work of pioneering researchers (Shimizu et al., 1984, 1985a; Fujiwara and Ogihara, 1986; Kida et al., 1997, 1998).

Materials and Methods

Chemicals and Reagents

SSa reference standard (purity, >98%) was purchased from the National Institutes for Food and Drug Control (Beijing, China). Analytical-grade ethyl carbamate was purchased from Sinopharm Chemical Reagent Co., Ltd. (Shanghai, China). High-performance LC–grade acetonitrile and methanol were purchased from Merck KGaA (Darmstadt, Germany). Analytical-grade Tween 80 was purchased from Tianjin Guangfu Fine Chemical Research Institute (Tianjin, China). Analytical-grade ethyl acetate was purchased from Nanjing Chemical Reagent Co., Ltd. (Nanjing, China). Twice-distilled water prepared in-laboratory was used throughout the study.

Dosing Procedure

Male Sprague-Dawley rats weighing 220 ± 20 g were purchased from the Qinglongshan Experimental Animal Center (Nanjing, China). The animals were housed under standard conditions with food and water provided ad libitum. Animal studies were conducted under the approval of the Animal Ethics Committee of the China Pharmaceutical University.

After acclimating in stainless steel rat metabolism cages individually for 1 week, the animals were fasted for 12 hours with free access to water before the experiment. SSa dissolved in 5% Tween 80 was administrated either i.v. via the tail vein at a dose of 15 mg/kg or through intragastric gavage at a dose of 50 mg/kg. The vehicle with equal volumes was administrated by either i.v. injection or intragastric gavage to the remaining half of the animals as the control.

Sample Collection

Plasma Collection. Twelve rats were divided into four groups with three animals per group. Blood samples (about 0.5 ml) were collected in 1.5 ml sodium heparinized tubes 0.083, 0.167, 0.333, 0.5, 1, 1.5, 3, 4.5, 6, 7.5, 9, 10.5, and 12 hours after i.v. or oral administration of the SSa or vehicle. Plasma samples of each animal were separated by centrifugation at 3000*g* for 10 minutes at 4°C in an Eppendorf centrifuge 5430 R (Eppendorf, Hamburg, Germany) and pooled over 0.083 to12 hours.

Bile Collection. Twelve rats divided into four groups with three animals per group were implanted with a PE-10 cannula (Smith Medical, Ashford, UK) into the bile duct under anesthesia by ethyl carbamate. Bile samples of each animal were collected on ice and pooled over 0 to 24 hours after i.v. or oral administration of the SSa or vehicle.

Urine and Feces Collection. The urine and feces were collected separately on ice over 0 to 24 hours from another 12 rats after i.v. or oral administration of the SSa or vehicle.

All of the collected plasma, bile, urine, and feces samples were stored at −20°C before analysis.

Sample Preparation

Plasma (2 ml) was loaded on the C18 cartridge (250 mg), washed with 5 ml water, and eluted with 3 ml acetonitrile. After the evaporation of the combined acetonitrile under a stream of nitrogen gas in water bath at 35°C, the residue was dissolved in 500 μl acetonitrile-water solution (50:50 [v/v]) for LC-DAD-IT-TOF-MS analysis. The bile and urine samples were treated by the same procedure as the plasma samples.

The feces specimens (0.5 g) were homogenized in 5 ml ice-cold acetonitrile-water solution [50:50 (v/v)] by a homogenizer (Shanghai Jinda Biochemical Equipment Co. Ltd., Shanghai, China). The homogenate was centrifuged at 2130*g* for 10 minutes to separate the supernatant, which was extracted with three times its volume of ethyl acetate. After centrifugation at 2130*g* for 10 minutes, the ethyl acetate layer was separated and vaporized under a stream of nitrogen gas in water bath at 35°C. The residue was dissolved in 500 μl acetonitrile-water solution (50:50 [v/v]) for LC-DAD-IT-TOF-MS analysis.

LC-DAD-IT-TOF-MS Analysis

LC experiments were conducted on a Shimadzu (Kyoto, Japan) high-performance LC system consisting of an LC-30AD binary pump, a DGU-20As degasser, a SIL-30AC autosampler, and a CTO-20AC column oven. Chromatographic separation was achieved on a Shimadzu VP-ODS column (150 mm × 2.0 mm, 2.2 μm) (Shimadzu) at 40°C. The mobile phase (delivered at 0.4 ml/min) comprised solvent A, acetonitrile-methanol solution (80:20 [v/v]), and solvent B, 0.06% HCOOH in water. A gradient elution was performed: 20–40% A for 0–20 minutes, 40–50% A for 20–60 minutes, 95% A for 60–70 minutes, and 20% A for 70–90 minutes. The UV absorption from 190 to 400 nm was recorded by an SPD-M20A diode array detector (Shimadzu) to determine whether the allyl oxide linkage in the 13,28 position of the aglycone moiety was broken into a heteroannular or homoannular diene (Kubota et al., 1966; Kubota and Hinoh, 1968).

MS analyses were conducted on a Shimadzu IT-TOF-MS (Shimadzu, Kyoto, Japan) equipped with an electrospray ionization source. MS^1 analysis was carried out in positive and negative mode simultaneously, followed by MS^n analyses in positive mode and MS^n analyses in negative mode, respectively. Some important equipment parameters were as follows: electrospray voltage, +4.5 kV for positive mode and −3.5 kV for negative mode; nebulizer gas (N_2) flow, 1.5 l/min; curved desolvation line temperature, 200°C; heat block temperature, 200°C; drying gas (N_2) pressure, 100 kPa; detector voltage, 1.7 kV; ion accumulated time, 50 milliseconds; positive scan range [mass-to-charge ratio (m/z)], 350–1350 for MS^1 and 100–900 for MS^2; negative scan range (m/z), 350–1350 for MS^1, 300–1000 for MS^2, and 200–800 for MS^3; collision energy, 30% both for positive and negative MS^n. After the data acquisition, MetID solution 1.2 (Shimadzu) was used to screen metabolite candidates. SSa, PSGf, and SGf were chosen as three templates in the mass defect filter method (Zhu et al., 2006; Zhang et al., 2009) with a mass defect window of ±0.050 Da.

Results

Fragment Pattern of SSa

At first, both the positive and negative MS fragment patterns of SSa were analyzed. Besides the typical adduct ion $[M+K]^+$ at m/z 819.4267 ($C_{42}H_{68}KO_{13}$) and $[M+Na]^+$ at m/z 803.4572 ($C_{42}H_{68}NaO_{13}$), we observed a large amount of fragment ions such as $[M-H_2O+H]^+$ at m/z 763.4635 ($C_{42}H_{67}O_{12}$), $[M-2H_2O+H]^+$ at m/z 745.4511 ($C_{42}H_{65}O_{11}$), $[M-H_2O\text{-glc}+H]^+$ (glc, glucose) at m/z 601.4083 ($C_{36}H_{57}O_7$), $[M-2H_2O\text{-glc}+H]^+$ at m/z 583.3982 ($C_{36}H_{55}O_6$), $[M-H_2O\text{-glc-fuc}+H]^+$ (fuc, fucose) at m/z 455.3534 ($C_{30}H_{47}O_3$), and $[M-2H_2O\text{-glc-fuc}+H]^+$ at m/z 437.3402 ($C_{30}H_{45}O_2$, 100% relative signal intensity) in the positive full-scan mass spectrum. Further, it was confirmed that 455.3534 comes from 763.4635 rather than 803.4572 or 819.4267 after comparing the MS^2 spectra of the precursor ions at m/z 763.4635, 803.4572, and 819.4267. The MS^2 spectrum obtained from the precursor ion at m/z 455.3458 showed 437.3398 ($C_{30}H_{45}O_2$, 455-H_2O), 419.3295 ($C_{30}H_{43}O$, 455-2H_2O), 401.3224 ($C_{30}H_{41}$, 455-3H_2O), 425.3399 ($C_{29}H_{45}O_2$, 455-CH_2O, McLafferty rearrangement), 407.3296 ($C_{29}H_{43}O$, 455-CH_2O-H_2O), and 389.3199 ($C_{29}H_{41}$, 455-CH_2O-2H_2O) in the high-m/z range. More importantly, in the low-m/z range appeared the characteristic fragment ions at m/z 223.1687 ($C_{14}H_{23}O_2$, named L1, ring C cleavage), 205.1584 ($C_{14}H_{21}O$, L1-H_2O), and 187.1484 ($C_{14}H_{19}$, L1-2H_2O, 100% relative signal intensity) corresponding to the AB ring (ABCDE were labelled on the structure of ion at m/z 763 in Fig. 2.) part; and those coming from the CDE ring part such as 299.2361 ($C_{21}H_{31}O$, named R1, ring B cleavage); 285.2213 ($C_{20}H_{29}O$, named R2, ring B cleavage), 267.2123 ($C_{20}H_{27}$, R2-H_2O); 283.2049 ($C_{20}H_{27}O$, named R3, ring B cleavage), 265.1946 ($C_{20}H_{25}$, R3-H_2O); 271.2073 ($C_{19}H_{27}O$, named R4, ring B cleavage), 253.1961 ($C_{19}H_{25}$, R4-H_2O), 241.1945 ($C_{18}H_{25}$, R4-CH_2O), 245.1915 ($C_{17}H_{25}O$, R4-C_2H_2, retro-Diels-Alder reaction),

Downloaded from dmd.aspetjournals.org at Zhejiang University on May 1, 2013

227.1687 ($C_{17}H_{23}$, R4-C_2H_2-H_2O); 269.1914 ($C_{19}H_{25}O$, named R5), 251.1805 ($C_{19}H_{23}$, R5-H_2O), 239.1811 ($C_{18}H_{23}$, R5-CH_2O); 233.1897 ($C_{16}H_{25}O$, named R6), 215.1789 ($C_{16}H_{23}$, R6-H_2O); and 231.1755 ($C_{16}H_{23}O$, named R7, ring C cleavage), 213.1648 ($C_{16}H_{21}$, R7-H_2O), 201.1634 ($C_{15}H_{21}$, R7-CH_2O), 205.1584 ($C_{14}H_{21}O$, R7-C_2H_2, retro-Diels-Alder reaction, coincided with L1-H_2O), 187.1484 ($C_{14}H_{19}$, R7-C_2H_2-H_2O, coincided with L1-H_2O) (see Fig. 1). The mass fragmentation pathway is proposed in Fig. 2.

In the negative full-scan mass spectrum, two major ions, the $[M+HCOO]^-$ at m/z 825.4654 ($C_{43}H_{69}O_{15}$, 100% relative signal intensity) and the $[M-H]^-$ at m/z 779.4593 ($C_{42}H_{67}O_{13}$), were observed. The anionic-adduct molecular ion transitioned to the predominant $[M-H]^-$ at m/z 779.4566 ($C_{42}H_{67}O_{13}$) in the MS^2 spectrum, which in turn gave the basic $[M\text{-glc-H}]^-$ at m/z 617.4067 ($C_{36}H_{57}O_8$) in the MS^3 spectrum. In the MS^4 experiment, isolation and fragmentation of 617.4067 resulted in the $[M\text{-glc-fuc-H}]^-$ at m/z 471.3464 ($C_{30}H_{47}O_4$, 100% relative signal intensity), the $[M\text{-glc-fuc-CH}_3\text{OH-H}]^-$ at m/z 439.3207 ($C_{29}H_{43}O_3$), and the one involving the ring-cross cleavage of fucose at m/z 541.3513 ($C_{33}H_{49}O_6$). This fragmentation was in agreement with the previous findings (Huang et al., 2008).

The positive and negative MS^n analysis was applied to identify the structures of the aglycone part and glycosyl group, respectively, in this experiment.

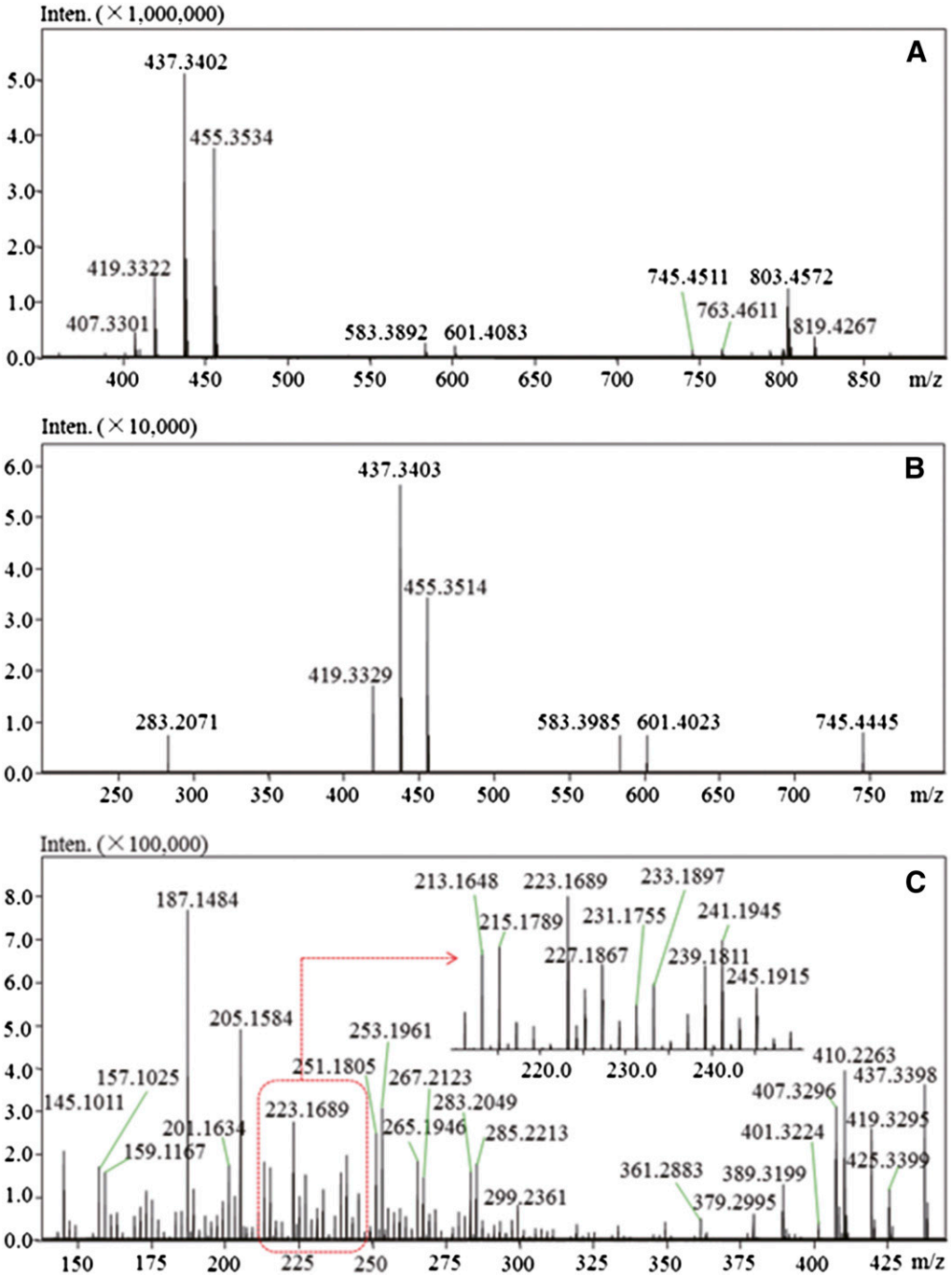

Fig. 1. The positive MS^n spectra of SSa. (A) Full-scan mass spectrum; (B) MS^2 of the precursor ion at m/z 763.4635; (C) MS^2 of the precursor ion at m/z 455.3534.

DMD DRUG METABOLISM AND DISPOSITION aspet

Downloaded from dmd.aspetjournals.org at Zhejiang University on May 1, 2013

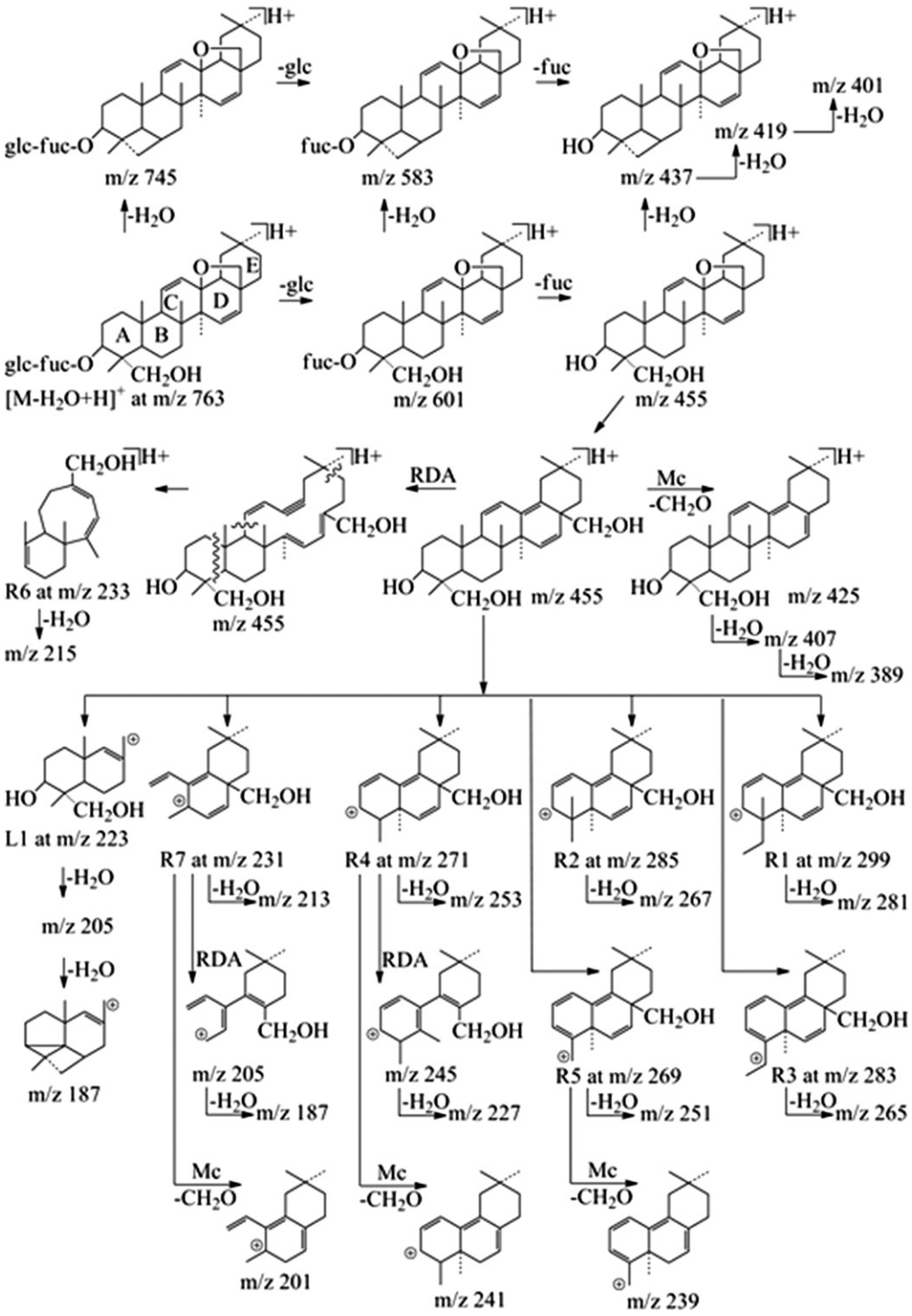

Fig. 2. Proposed fragmentation pathway of SSa.

Screening of Metabolites

With the aid of the MetID solution 1.2 software, the metabolites were screened by comparing the full-scan mass spectra of the plasma, bile, urine, and feces of rats after administration of SSa with that of the control samples of rats after administration of vehicle. A total of 17 metabolites were detected besides the parent drug. The extracted ion chromatograms of the typical biosamples are shown in Fig. 3. Information on the parent compound and metabolites is summarized in Tables 1 and 2.

Structure Elucidation of Metabolites

M0 (Parent Drug). M0 in samples was unambiguously identified by comparing the retention time and MS and UV data with the standard reference.

M13 (Hydration). Based on the $[M+Na]^+$ at m/z 821.4632 ($C_{42}H_{70}NaO_{14}$) in the positive full-scan mass spectrum and the $[M-H]^-$ at m/z 797.4706 ($C_{42}H_{69}O_{14}$) and the $[M+HCOO]^-$ at m/z 843.4772 ($C_{43}H_{71}O_{16}$, 100% relative signal intensity) in the negative full-scan mass spectrum, the molecular formula (MF) of M13 was

DMD
DRUG METABOLISM AND DISPOSITION
aspet
Downloaded from dmd.aspetjournals.org at Zhejiang University on May 1, 2013

DMD DRUG METABOLISM AND DISPOSITION aspet

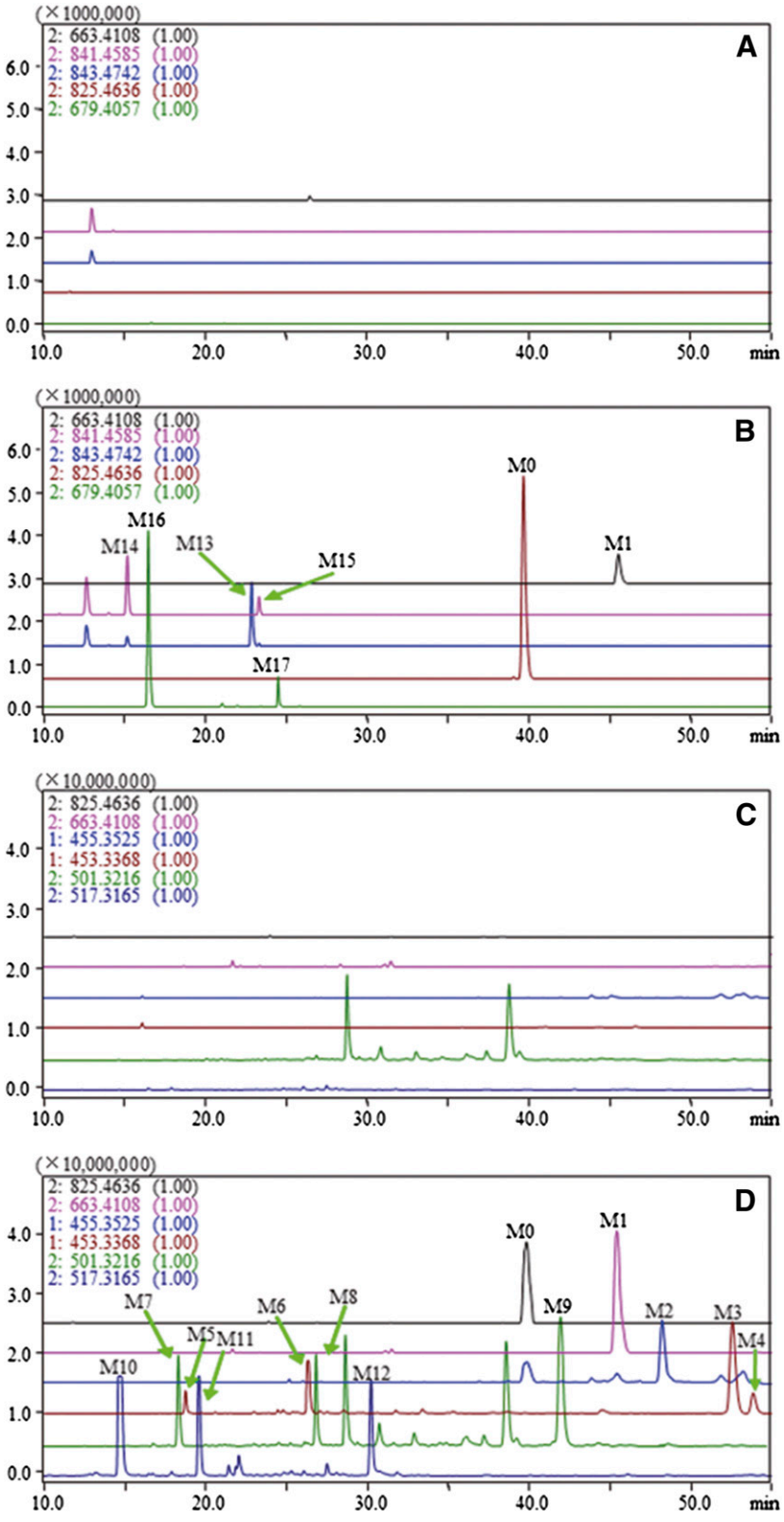

Fig. 3. Extracted ion chromatograms of the typical biosamples of rats. (A) Control bile sample after i.v. administration; (B) drug-containing bile sample after i.v. administration; (C) control feces sample after oral administration; (D) drug-containing feces sample after oral administration.

determined as $C_{42}H_{70}O_{14}$, with one H_2O more than M0. The MS^2 spectrum of deprotonated molecular ion showed the predominant $[M\text{-glc-H}]^-$ at m/z 635.4135 ($C_{36}H_{59}O_9$), which subsequently provided the major fragment ions including the $[M\text{-glc-fuc-H}_2O\text{-H}]^-$ at m/z 471.3479 ($C_{30}H_{47}O_4$, 100% relative signal intensity), the $[M\text{-glc-fuc-H}_2O\text{-CH}_3OH\text{-H}]^-$ at m/z 439.3214 ($C_{29}H_{43}O_3$), and the one involving ring-cross cleavage of the fucose moiety at m/z 559.3655 ($C_{33}H_{51}O_7$) in the MS^3 spectrum. This fragment pattern was identical to that of hydroxysaikosaponin a (HOSSa) as reported previously (Huang et al., 2008). Further, we validated this inference by comparison of its retention time with that of HOSSa derived from SSa in aqueous condition. Thus M13 was identified as HOSSa. The conversion of SSa

Downloaded from dmd.aspetjournals.org at Zhejiang University on May 1, 2013

TABLE 1

Metabolites of SSa detected by the MD filter method with different templates

MD Filter Template	Metabolites	MF	Mol. Wt.	ΔMD from Template	Metabolites' Appearance in Biosamples							
					I.V.				Oral			
					Plasma	Bile	Urine	Feces	Plasma	Bile	Urine	Feces
			Da									
SSa	M0	$C_{42}H_{68}O_{13}$	780.4660	0	+	+	+	–	+	+	+	+
	M13	$C_{42}H_{70}O_{14}$	798.4765	0.0106	–	+	–	–	–	–	–	–
$C_{42}H_{68}O_{13}$, 780.4659	M14	$C_{42}H_{68}O_{14}$	796.4609	−0.0050	–	+	–	–	–	+	–	–
	M15	$C_{42}H_{68}O_{14}$	796.4609	−0.0050	–	+	–	–	–	–	–	–
PSGf	M1	$C_{36}H_{58}O_8$	618.4131	0	+	+	+	+	+	+	+	+
$C_{36}H_{58}O_8$, 618.4131	M16	$C_{36}H_{58}O_9$	634.4080	−0.0051	–	+	–	–	–	+	–	–
	M17	$C_{36}H_{58}O_9$	634.4080	−0.0051	–	+	–	–	–	–	–	–
SGf	M2	$C_{30}H_{48}O_4$	472.3552	0	–	–	–	+	–	–	+	+
$C_{30}H_{48}O_4$, 472.3552	M3	$C_{30}H_{46}O_4$	470.3396	−0.0156	–	–	–	–	–	–	+	+
	M4	$C_{30}H_{46}O_4$	470.3396	−0.0156	–	–	–	–	–	–	+	+
	M5	$C_{30}H_{48}O_5$	488.3501	−0.0051	–	–	–	+	–	–	–	+
	M6	$C_{30}H_{48}O_5$	488.3501	−0.0051	–	–	–	+	–	–	–	+
	M7	$C_{30}H_{46}O_6$	502.3294	−0.0258	–	–	–	+	–	–	+	+
	M8	$C_{30}H_{46}O_6$	502.3294	−0.0258	–	–	–	+	–	–	+	+
	M9	$C_{30}H_{46}O_6$	502.3294	−0.0258	–	–	–	+	–	–	+	+
	M10	$C_{30}H_{46}O_7$	518.3243	−0.0309	–	–	–	+	–	–	+	+
	M11	$C_{30}H_{46}O_7$	518.3243	−0.0309	–	–	–	+	–	–	+	+
	M12	$C_{30}H_{46}O_7$	518.3243	−0.0309	–	–	–	–	–	–	+	+

MD, mass defect; MF, molecular formula; PSGf, prosaikogenin f; SGf, saikogenin f; SSa, saikosaponin a.
+, detected.
−, undetected.

to HOSSa, which can occur to a limited extent in aqueous solvent, may accelerate in vivo.

M14 and M15 (Monooxidation). From the $[M+Na]^+$ at m/z 819.4527 ($C_{42}H_{68}NaO_{14}$) in the positive full-scan mass spectrum and the $[M-H]^-$ at m/z 795.4561 ($C_{42}H_{67}O_{14}$) and the $[M+HCOO]^-$ at m/z 841.4623 ($C_{43}H_{69}O_{16}$, 100% relative signal intensity) in the negative full-scan mass spectrum, their MF was determined as $C_{42}H_{68}O_{14}$, with one oxygen more than M0. Their predominant fragment ion $[M-glc-H]^-$ at m/z 633.3976 ($C_{36}H_{57}O_9$) from the precursor ion at m/z 795.4561 in the MS^2 spectrum transitioned to the major fragment ion $[M-glc-fuc-H]^-$ at m/z 487.3436 ($C_{30}H_{47}O_5$, 100% relative signal intensity) in the MS^3 spectrum. In addition, the $[M-glc-fuc-CH_3OH-H]^-$ at m/z 455.3172 ($C_{29}H_{43}O_4$) and the one involving ring-cross cleavage of the fucose moiety at m/z 557.3457 ($C_{33}H_{49}O_7$) were also observed in the MS^3 spectrum of M14 but not M15. These data indicated that both M14 and M15 were monooxidative metabolites of SSa and the added oxygen should locate on the aglycone part. But we failed to assign the exact substitution.

M1 (Hydrolysis of β-Glucosidic Bond). According to the $[M-H_2O+H]^+$ at m/z 601.4077 ($C_{36}H_{57}O_7$) in the positive full-scan mass spectrum and the $[M-H]^-$ at m/z 617.4076 ($C_{36}H_{57}O_8$) and the $[M+HCOO]^-$ at m/z 663.4124 ($C_{37}H_{59}O_{10}$, 100% relative signal intensity) in the negative full-scan mass spectrum, the MF of M1 was determined as $C_{36}H_{58}O_8$. The similar positive MS^2 spectrum of the precursor ion at m/z 455.3541 to that of the parent compound indicated that M1 has the same aglycone as SSa, which was confirmed by its UV end absorption. The same negative MS/MS spectrum of the precursor ion at m/z 617.4076 as that of the parent compound showed the linkage of a deoxyhexose to the aglycone. These spectral data were in agreement with those of PSGf as reported in the literature (Huang et al., 2008). M1 was identified as PSGf.

M16 and M17 (Monooxidation and Hydrolysis of β-Glucosidic Bond). The MF of M16 and M17 was determined as $C_{36}H_{58}O_9$, with one oxygen more than M1, according to the $[M+Na]^+$ at m/z 657.3997 ($C_{36}H_{58}NaO_9$) in the positive full-scan mass spectrum and the $[M-H]^-$ at m/z 633.4018 ($C_{36}H_{57}O_9$) and the $[M+HCOO]^-$ at m/z 679.4031 ($C_{37}H_{59}O_{11}$, 100% relative signal intensity) in the negative full-scan mass spectrum. The MS/MS spectrum of the precursor ion at m/z 633.4018 gave the major fragment ions including the $[M-fuc-H]^-$ at m/z 487.3447 ($C_{30}H_{47}O_5$, 100% relative signal intensity) and the $[M-fuc-CH_3OH-H]^-$ at m/z 455.3178 ($C_{29}H_{43}O_4$), while the one involving ring-cross cleavage of the fucose moiety at m/z 557.3489 ($C_{33}H_{49}O_7$) appeared in the MS^2 spectrum of M16 rather than M17. This fragmentation was very similar to that of M14 and M15. We supposed that M16 and M17 derived from M14 and M15, respectively, through hydrolyzing the terminal glucose moiety according to their MS^2 spectra and retention time.

M2 (Hydrolysis of β-Fucosidic Bond). The MF of M2 was determined as $C_{30}H_{48}O_4$ based on the $[M-H_2O+H]^+$ at m/z 455.3527 ($C_{30}H_{47}O_3$) in the positive full-scan mass spectrum and the $[M+HCOO]^-$ at m/z 517.3513 ($C_{31}H_{49}O_6$) in the negative full-scan mass spectrum. The similar positive MS^2 spectrum of the precursor ion at m/z 455.3527 to that of the parent compound suggested that M2 has the same aglycone as the parent compound, which was also confirmed by the UV end absorption. So M2 was identified as SGf as reported previously (Shimizu et al., 1985b).

M3 and M4 (Dehydrogenation and Hydrolysis of β-Fucosidic Bond). According to the $[M+Na]^+$ at m/z 493.3279 ($C_{30}H_{46}NaO_4$) and the $[M-H_2O+H]^+$ at m/z 453.3378 ($C_{30}H_{45}O_3$) in the positive full-scan mass spectrum, the MF of M3 and M4 was supposed as $C_{30}H_{46}O_4$, with two hydrogens fewer than M2. The CDE ring part structures of M3 and M4 remained intact according to the fragment ions at m/z 285.2207 ($C_{20}H_{29}O$, ion R2) and 267.2109 ($C_{20}H_{27}$, R2-H_2O) from the precursor ion at m/z 453.3378 in the MS^2 spectrum. Their fragment ions at m/z 221.1550 ($C_{14}H_{21}O_2$, named L2) and 203.1428 ($C_{14}H_{19}O$, L2-H_2O, 100% relative signal intensity) were 2 Da less than ion L1 and L1-H_2O, respectively. These results indicated that the dehydrogenation of both M3 and M4 took place on the AB ring part structure. The fragment ion of M3 at m/z 175.1479 ($C_{13}H_{19}$, L2-H_2O-CO) resulting from neutral loss of CO from 203.1428 suggested that M3 has a ketone carbonyl group on the ring that should locate at C3. So M3 was inferred as 3-keto-SGf. As to M4, the fragment ion at m/z

DMD DRUG METABOLISM AND DISPOSITION aspet
Downloaded from dmd.aspetjournals.org at Zhejiang University on May 1, 2013

TABLE 2

LC-DAD-IT-TOF-MS analysis of SSa and its observed metabolites in rat biosamples

No.	T_R	UV	Positive MS^1	Negative MS^1	Positive MS^n	Negative MS^n	Identity
	min	*nm*					
M0	39.9	<190	437.3402[a], 455.3534, 583.3982, 601.4083,745.4511, 763.4635,803.4572, 819.4267	779.4593, 815.4310, 825.4654[a], 842.4867, 893.4467	[763.4635] → 745.4532, 601.4123, 583.3985, 455.3514, 437.3403[a], 419.3329 [455.3534] → 437.3398, 425.3399, 419.3295, 407.3296, 401.3224, 389.3199, 299.2361, 285.2213, 283.2049, 267.2123, 265.1946, 253.1961, 251.1805, 241.1945, 239.1811, 233.1897, 231.1755, 223.1689, 215.1789, 213.1648, 205.1584, 201.1634, 187.1484[a]	[825.4654] → [779.4566[a]]→ [617.4067[a]] → 541.3513, 471.3464[a], 439.3207	SSa[b]
M13	22.9	<190	821.4632	797.4706 843.4772[a]		[797.4706] → [635.4135[a]] → 559.3655, 471.3479[a], 439.3214	HOSS[c]
M14	15.2	<190	819.4527	795.4561 841.4623[a]		[795.4561] → [633.3976[a]] → 557.3457, 487.3436[a], 455.3172	Monooxidation of SSa
M15	23.3	<190	819.4512	795.4553 841.4609[a]		[795.4553] → [633.3995[a]] → 487.3436[a]	Monooxidation of SSa
M1	45.5	<190	437.3425[a] 455.3541, 601.4077	617.4076 663.4124[a]	[455.3541] → 285.2224, 267.2106, 223.1687, 205.1587, 187.1478[a]	[617.4076[a]] → 541.3523, 471.3485[a], 439.3222	PSGf[c]
M16	16.5	<190	657.3997	633.4018 679.4031[a]		[633.4018] → 557.3489, 487.3447[a], 455.3178	Monooxidation of PSGf
M17	24.5	<190	657.3968	633.4029 679.4047[a]		[633.4029] → 487.3440[a], 455.3144	Monooxidation of PSGf
M2	48.3	<190	437.3411[a], 455.3527	517.3513[a]	[455.3527] → 285.2210, 267.2118, 223.1703, 205.1597, 187.1497[a]		SGf[c]
M3	52.3	<190	435.3271[a] 453.3378, 493.3279		[453.3378] → 423.3273[a], 393.3140, 285.2207, 267.2109, 233.1896, 221.1550, 215.1792, 203.1428, 175.1479		Δ^1-SGf
M4	53.7	<190	435.3254[a], 453.3372		[453.3372] → 285.2217, 267.2114, 221.1536, 203.1443[a], 185.1335		3-keto-SGf
M5	18.6	<190	453.3369[a], 471.3457	533.3499[a]	[471.3457] → 249.1861, 231.1739, 223.1697, 213.1651, 205.1601, 187.1489[a]		Hydroxylation of SGf
M6	26.0	<190	453.3361[a], 471.3469	533.3467[a]	[471.3469] → 453.3387[a] [453.3361] → 229.1584, 223.1693, 211.1477, 205.1591, 187.1487[a]		Hydroxylation of SGf
M7	18.4	<190	467.3153[a], 485.3250	501.3234[a]	[485.3250] → 455.3161, 263.1656, 245.1533, 231.1374, 223.1692, 205.1594, 199.1493, 187.1482[a]	[501.3234] → 453.2987[a], 437.3038	SGf-27-oic acid
M8	42.2	<190	467.3167[a], 485.3273	501.3238[a]	[485.3273] → 253.1451, 235.1340, 233.1907, 217.1224, 215.1805, 171.1169[a]	[501.3238] → 453.2991[a], 437.3044	Carboxylation and hydroxylation of SGf
M9	27.0	<190	467.3158[a], 485.3259	501.3217[a]	[485.3259] → 467.3140[a] [467.3158] → 449.3050[a], 431.2941	[501.3217] → 453.3016[a], 437.3069	Unidentified
M10	14.7	<190	483.3098[a], 501.3199	517.3171[a]	[501.3199] → 253.1447, 249.1867, 235.1345, 231.1743, 217.1235, 213.1635, 171.1167[a]	[517.3171] → 469.2965[a], 453.3023	Carboxylation and hydroxylation of SGf
M11	19.6	<190	483.3104[a], 501.3204	517.3152[a]	[501.3199] → 483.3127[a] [483.3104] → 465.3021[a]	[517.3152] → 469.2932[a], 453.2989	Unidentified
M12	30.2	<190	483.3123[a], 501.3207	517.3184[a]	[501.3207] → 483.3087[a] [483.3123] → 465.2983[a]	[517.3184] → 469.2936[a], 453.2991	Unidentified

HOSS, hydroxysaikosaponin; LC-DAD-IT-TOF-MS, liquid chromatography–diode array detector coupled with hybrid ion trap–time-of-flight mass spectrometry; PSGf, prosaikogenin f; SGf, saikogenin f; SSa, saikosaponin a.

[a] Of 100% relative signal intensity.

[b] With standard.

[c] With data in reference.

DMD DRUG METABOLISM AND DISPOSITION aspet

Downloaded from dmd.aspetjournals.org at Zhejiang University on May 1, 2013

185.1335 ($C_{14}H_{17}$, L3-2H_2O) with 2 Da less than L1-2H_2O indicated that the dehydrogenation of M4 could only have occurred on ring A with two hydroxyl groups remaining. Most likely, M4 should be Δ^1-SGf. Some key MS fragmentation of M3 and M4 is proposed in Fig. 4, A and B, respectively.

M5 and M6 (Hydroxylation and Hydrolysis of β-Fucosidic Bond). The MF of M5 and M6 was determined as $C_{30}H_{48}O_5$, with one oxygen more than M2 from the $[M\text{-}H_2O+H]^+$ at m/z 471.3457 ($C_{30}H_{47}O_4$) and the $[M\text{-}2H_2O+H]^+$ at m/z 453.3369 ($C_{30}H_{45}O_3$, 100% relative signal intensity) in the positive full-scan mass spectrum and the $[M+HCOO]^-$ at m/z 533.3499 ($C_{31}H_{49}O_7$) in the negative full-scan mass spectrum. Their AB ring part structure didn't change according to the fragment ions at m/z 223.1697 ($C_{14}H_{23}O_2$, L1), 205.1601 ($C_{14}H_{21}O$, L1-H_2O), and 187.1489 ($C_{14}H_{19}$, L1-2H_2O, 100% relative signal intensity) in the MS^2 spectrum of the precursor ion at m/z 471.3457 of M5 and 453.3369 of M6. The fragment ions of

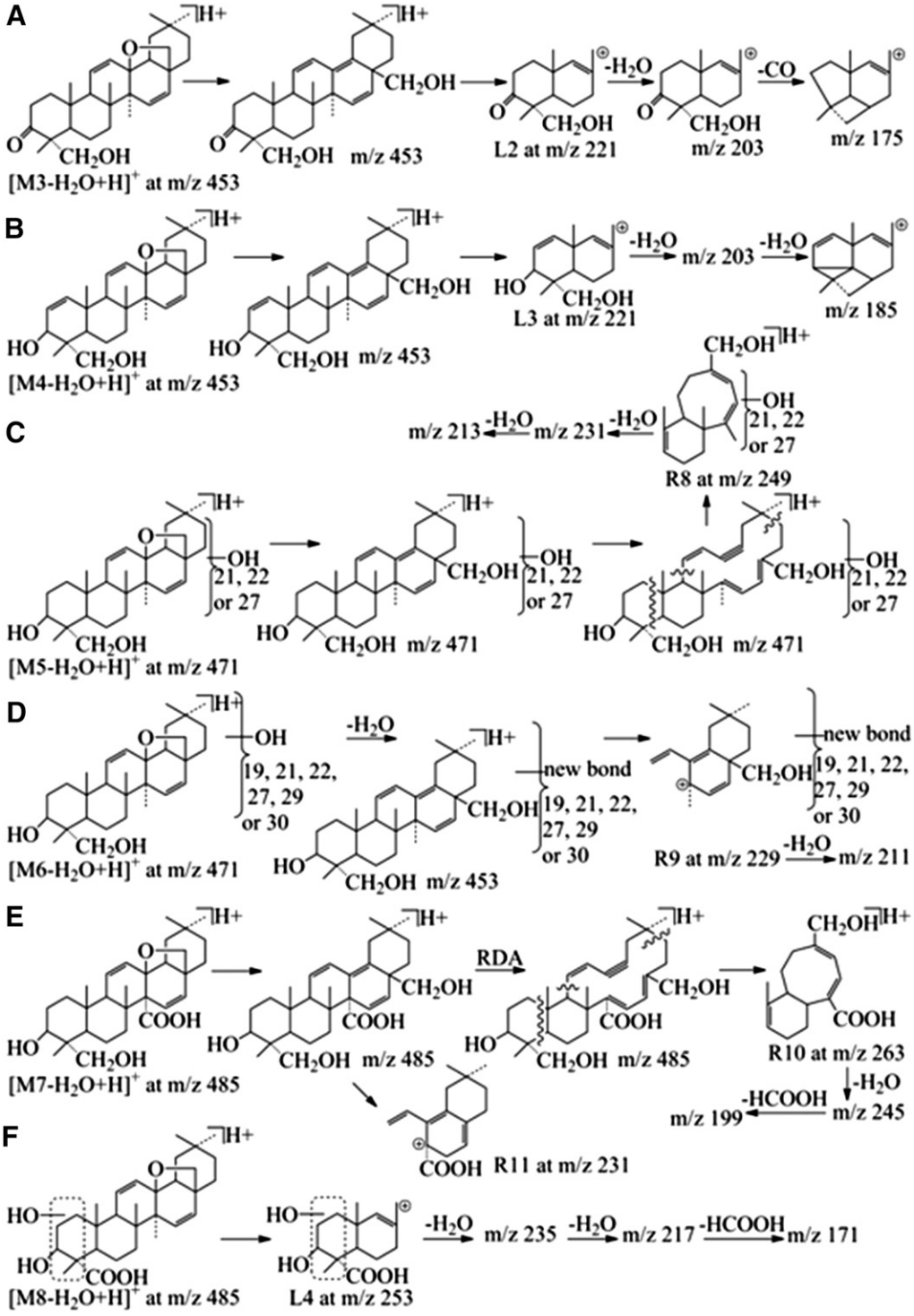

Fig. 4. Proposed fragmentation pathways of part of metabolites. (A) M3; (B) M4; (C) M5; (D) M6; (E) M7; (F) M8.

DMD
DRUG METABOLISM AND DISPOSITION
aspet
Downloaded from dmd.aspetjournals.org at Zhejiang University on May 1, 2013

M5 at m/z 249.1861 ($C_{16}H_{25}O_2$, named R8), 231.1739 ($C_{16}H_{23}O$, R8-H_2O), and 213.1651 ($C_{16}H_{21}$, R8-2H_2O) resulting from the precursor ion [M-H_2O+H]$^+$ at m/z 471.3457 were in agreement with R6+O, R6 +O-H_2O, and R6+O-2H_2O, respectively. We supposed that hydroxylation occurred on the CDE ring part structure of M5 and the introduced hydroxyl function may locate at C21, C22, or C27. The key MS fragmentation of M5 is illustrated in Fig. 4C. For M6, the fragment ions at m/z 229.1584 ($C_{16}H_{21}O$, named R9) and 211.1477 ($C_{16}H_{19}$, R9-H_2O) obtained from the precursor ion [M-2H_2O+H]$^+$ at m/z 453.3369 were consistent with R7+O-H_2O and R7+O-2H_2O, respectively, indicating that hydroxylation took place on the CDE ring part structure of M6 and the added hydroxyl group may be at C19, C21, C22, C27, C29, or C30. The key MS fragmentation of M6 is shown in Fig. 4D.

M7(Carboxylation and Hydrolysis of β-Fucosidic Bond). Based on the [M-H_2O+H]$^+$ at m/z 485.3250 ($C_{30}H_{45}O_5$) and the [M-2H_2O+H]$^+$ at m/z 467.3153 ($C_{30}H_{43}O_4$, 100% relative signal intensity) in the positive full-scan mass spectrum and the [M-H]$^-$ at m/z 501.3234 ($C_{30}H_{45}O_6$) in the negative full-scan mass spectrum, the MF of M7 was determined as $C_{30}H_{46}O_6$, with two oxygens more and two hydrogens fewer than M2. In the MS^2 spectrum of the precursor ion at m/z 485.3250, the fragment ions at m/z 223.1692 ($C_{14}H_{23}O_2$, L1), 205.1594 ($C_{14}H_{21}O$, L1-H_2O), and 187.1482 ($C_{14}H_{19}$, L1-2H_2O, 100% relative signal intensity) showed the intact AB ring part structure. Moreover, the fragment ions at m/z 263.1567 ($C_{16}H_{23}O_3$, named R10, in line with R6+2O-2H), 245.1433 ($C_{16}H_{21}O_2$, R10-H_2O), and 199.1510 ($C_{15}H_{19}$, R10-H_2O-HCOOH) showed one carboxyl function and two hydroxyl groups on the CDE ring part structure and eliminated the possibility of carboxylation at C29 or C30. The end absorption in UV spectrum ruled out the possibility of carboxylation at C28, which otherwise needed the 13,28-oxide bridge to break into a heteroannular or homoannular diene. Taken together, M7 was tentatively characterized as SGf-27-oic acid, and its key MS fragmentation is presented in Fig. 4E.

M8 and M10 (Hydroxylation, Carboxylation, and Hydrolysis of β-Fucosidic Bond). As an isomer of M7, the MF of M8 was also determined as $C_{30}H_{46}O_6$, with two oxygens more and two hydrogens fewer than M2, based on the positive and negative full-scan mass spectra. The CDE ring part structure of this metabolite remained unchanged according to its fragment ions at m/z 233.1907 ($C_{16}H_{25}O$, R6) and 215.1805 ($C_{16}H_{23}$, R6-H_2O) from the precursor ion at m/z 485.3273 in the MS^2 spectrum. Additionally, the fragment ions at m/z 253.1451 ($C_{14}H_{21}O_4$, named L4, consistent with L1+2O-2H), 235.1340 ($C_{14}H_{19}O_3$, L4-H_2O), 217.1224 ($C_{14}H_{17}O_2$, L4-2H_2O), and 171.1169 ($C_{13}H_{15}$, L4-2H_2O-HCOOH, 100% relative signal intensity) suggested that carboxylation happened on the AB ring part

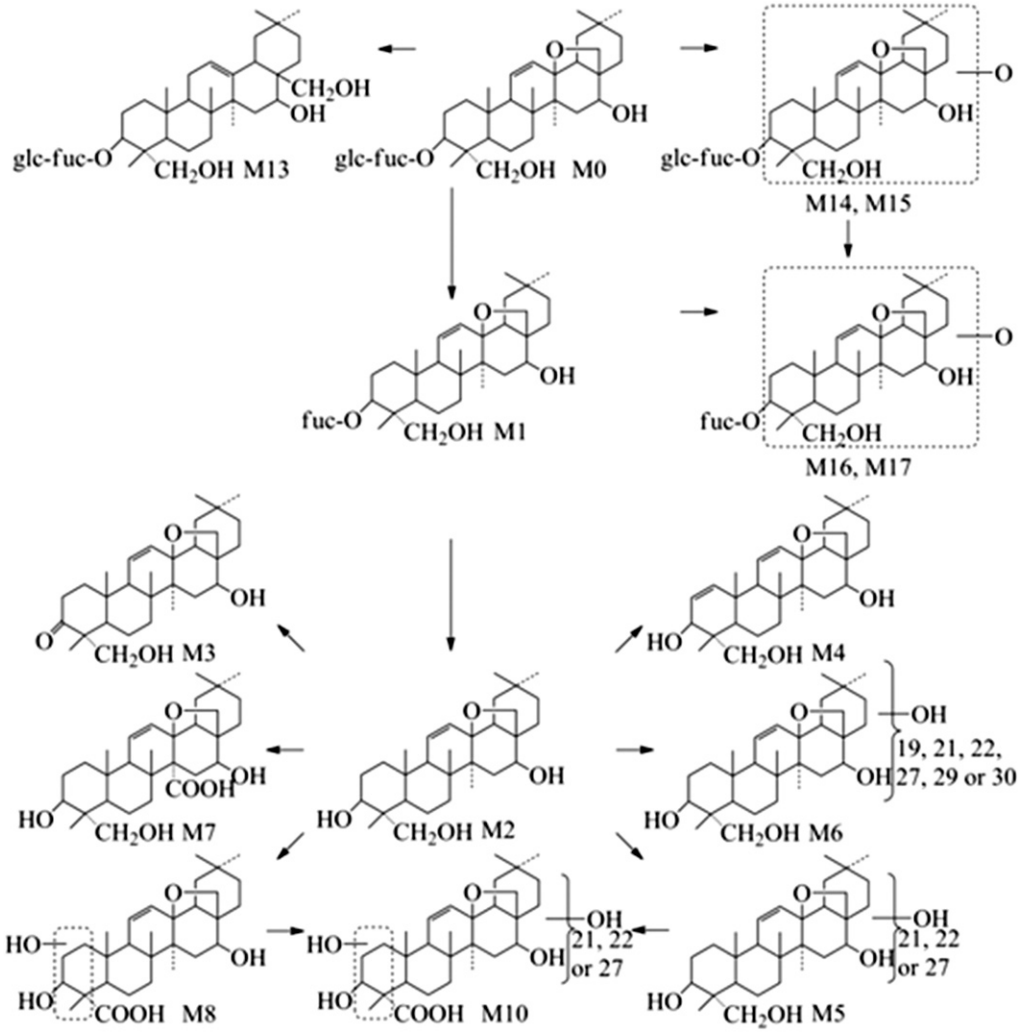

Fig. 5. The major metabolic pathway of SSa in rats.

DMD DRUG METABOLISM AND DISPOSITION aspet
Downloaded from dmd.aspetjournals.org at Zhejiang University on May 1, 2013

structure. Further, the carboxyl group should not locate at C25 or C26 because of the fragment ions at m/z 233.1907 ($C_{16}H_{25}O$, R6) and 215.1805 ($C_{16}H_{23}$, R6-H_2O) responsible for the CDE ring part structure. We supposed that carboxylation took place at 23-CH_2OH, accompanied by hydroxylation at C1, C2, or C24. The key MS fragmentation of M8 is illustrated in Fig. 4F.

The MF of M10 was determined as $C_{30}H_{46}O_7$, with three oxygens more and two hydrogens fewer than M2 according to the $[M\text{-}H_2O+H]^+$ at m/z 501.3199 ($C_{30}H_{45}O_6$) and the $[M\text{-}2H_2O+H]^+$ at m/z 483.3980 ($C_{30}H_{43}O_5$, 100% relative signal intensity) in the positive full-scan mass spectrum and the $[M-H]^-$ at m/z 517.3171 ($C_{30}H_{45}O_7$) in the negative full-scan mass spectrum. In the MS^2 spectrum of the precursor ion at m/z 501.3199, the major fragment ions at m/z 253.1447 ($C_{14}H_{21}O_4$, L4), 235.1345 ($C_{14}H_{19}O_3$, L4-H_2O), 217.1235 ($C_{14}H_{17}O_2$, L4-2H_2O), and 171.1167 ($C_{13}H_{15}$, L4-2H_2O-HCOOH, 100% relative signal intensity) suggested that M10 has the same AB ring part structure as M8, while the fragment ions at m/z 249.1584 ($C_{16}H_{25}O_2$, R8), 231.1713 ($C_{16}H_{23}O$, R8-H_2O), and 213.1560 ($C_{16}H_{21}$, R8-2H_2O) indicated that it has the same CDE ring part structure as M5.

The accurate mass data with error (ppm) for fragment ions of all metabolites are listed in Supplemental Table 1.

Discussion

The main objective of the present study was to completely characterize the metabolites of the triterpenoid SSa in rats. To this aim, we compared the metabolites in plasma, bile, urine, and feces samples following oral and i.v. routes of administration. Our results showed that SSa is metabolized diversely. The metabolic profile is proposed in Fig. 5. The observed routes of SSa metabolism are some types of oxidation such as dehydrogenation, hydroxylation, carboxylation, and combinations of these steps on the aglycone moiety, in addition to the previously reported hydrolysis of glycosidic bonds (Shimizu et al., 1985a; Kida et al., 1998).

The detected metabolites in biosamples differ via different routes of administration, as summarized in Table 1. So a relative comprehensive information of in vivo experience of SSa was deduced from the complementary results after different routes of administration, as shown in Fig. 6. After intravenous dosing, SSa was oxidized into M14 and M15 in the liver, as indicated by their detection in the bile. Interestingly, the β-glucosidic bond of SSa, M14, and M15 was hydrolyzed to produce M1, M16, and M17, respectively, as detected in the bile, suggesting that the hydrolyzing activity for the β-glucosidic bond exists not only in the intestinal bacteria but also in the liver. This inference is supported by other reports that various soluble and membrane-bound β-glucosidase with broad specificity catalyzing such reactions had been detected in most mammalian tissues (Robinson, 1956; Abrahams and Robinson, 1969; Glew et al., 1976; Daniels et al., 1981). SSa and M13–M17 excreted through the bile duct were metabolized further in the intestine, according to their disappearance in the feces. In the intestine, SSa was metabolized through hydrolysis mediated by the intestinal flora following oxidation catalyzed by the metabolizing enzymes in the intestinal mucosal cells (Kaminsky and Zhang, 2003; Zhang et al., 2007). Both the renal and biliary routes were observed for the excretion of SSa and its metabolites. In the case of oral administration, M1–M4 and M7–M12 produced in the intestine were partly absorbed into the systemic circulation, as indicated by their excretion in the urine. This may be due to their improved permeability through the intestinal membrane after hydrolysis of glycosidic bonds because the permeability decreased in the order of saikogenin a, prosaikogenin a, and saikosaponin b1, as reported previously (Kida et al., 1998). Additionally, our results showed that no saikosaponin b1 or g, prosaikogenin a or h, or saikogenin a or h was detected in all the biosamples after oral administration of SSa, suggesting the negligible effect of gastric juice on the allyl oxide linkage in the 13,28 position, which was consistent with the findings of Shimizu et al. (1985a).

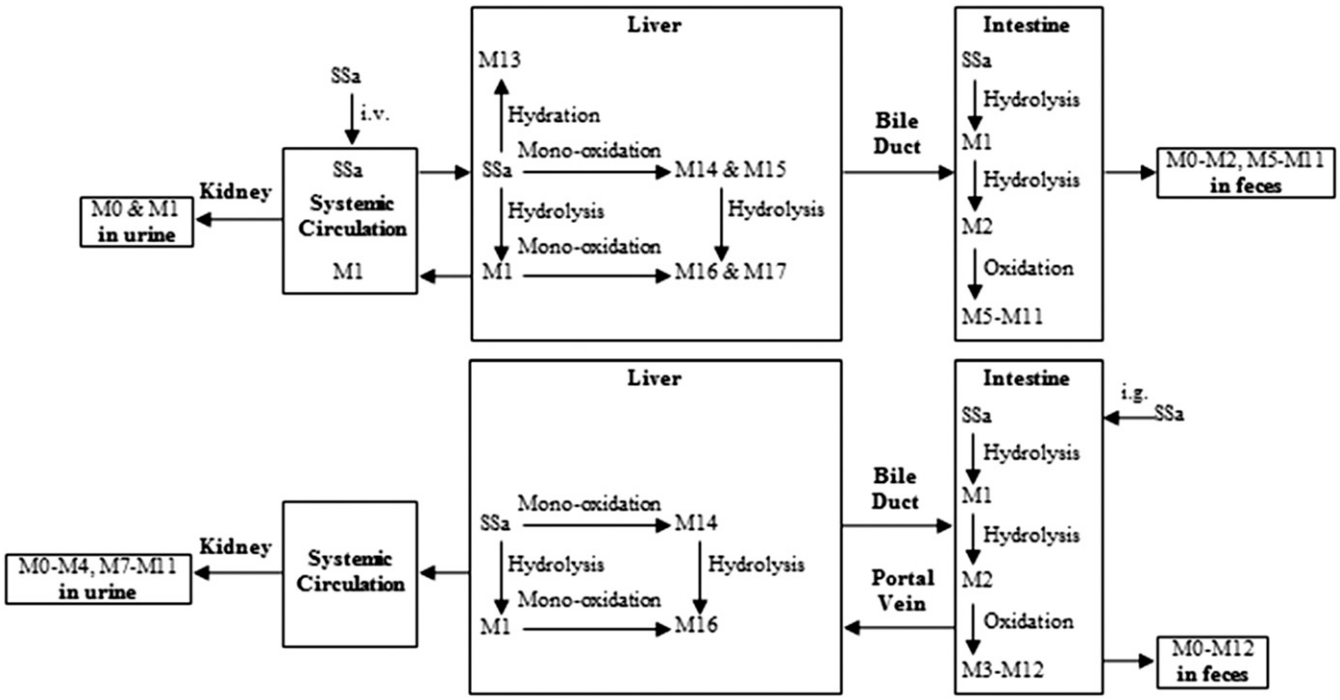

Fig. 6. The proposed disposition of SSa in rats after oral and i.v. administration.

DMD DRUG METABOLISM AND DISPOSITION aspet
Downloaded from dmd.aspetjournals.org at Zhejiang University on May 1, 2013

DMD DRUG METABOLISM AND DISPOSITION aspet

Furthermore, various bioactivities of saikosaponins might be linked closely to their interaction with biomembranes of cells which appeared to intimately parallel their degree of hemolytic activity (Ahn and Sok, 2006). Previous structure-activity relationship research showed that for these activities the ether linkage between C13 and C28, the 23-CH_2OH, the configuration of the hydroxyl group at C16, and the proper polar balance between the sugar moiety (polar position) and the aglycone moiety (nonpolar position) are important (Abe et al., 1980; Yokoyama et al., 1981; Nose et al., 1989a,b; Kumazawa et al., 1990; Ahn et al., 1998; Tsai et al., 2002). In this experiment, the ether linkage between C13 and C28 of all identified metabolites except M13 didn't cleave according to their UV spectra. The configuration of the hydroxyl group at C16 of SSa was β type and so should be that of its metabolites. The polar balance of metabolites had been broken after the hydrolysis of glycosidic bonds but was compensated to some degree by the addition of hydroxyl and carboxyl groups on the aglycone moiety. It is believed that the addition of functional groups such as –OH, –COOH, –SH, –O–, or $–NH_2$ by the phase I enzymes can dramatically alter the biologic properties of the drug (Brunton et al., 2008). As to saikosaponins, the –OH was proven important for their interaction with the cell surface based on the fact that whereas the transformation of the 23-methyl group (saikosaponin e) to CH_2OH (SSa) resulted in twofold enhancement in the anti–cell adhesive activity on the whole, the acetylation of this carbinol group to form 23-*O*-acetylsaikosaponin-a led to a substantial loss of action (Ahn et al., 1998). Thus, the introduction of the hydroxyl and carboxyl group on the aglycone moiety may lead to the marked change of activities, which is of significance for the development of saikosaponins in the pharmaceutical industry. In addition, we also detected two dehydrogenating metabolites, M3 and M4, in both the feces and urine of rats after oral dosing of SSa. The addition of unsaturated group on M3 and M4 may make them function as electrophiles that can react with nucleophilic cellular macromolecules such as DNA, RNA, and protein. Further assessment of the exposure and activities of these metabolites still needs to be conducted.

To summarize, the metabolic profile of SSa in rats has been characterized in detail by comparing the results following different routes of administration using LC-DAD-IT-TOF-MS. The observed routes of SSa metabolism involve hydration and monooxidation on the aglycone moiety and hydrolysis of the β-glucosidic bond in the liver and various types of oxidation including dehydrogenation, hydroxylation, and carboxylation on the aglycone moiety following sequential hydrolysis of both β-glucosidic and β-fucosidic bonds in the intestinal tract. SSa and its metabolites can be excreted through both the renal and biliary routes. These results may provide valuable information for assessing the efficacy and safety of clinical applications of prescriptions containing saikosaponins. Moreover, the discussion of oxidation on the aglycone moiety gives us some clues for structural modification of these promising compounds.

Acknowledgments

The authors thank Jinting Yao and Luying Zhou from Analytical Applications Center, Analytical Instruments Department, Shimadzu (China) Co., Ltd., for guidance in the operation of IT-TOF-MS.

Authorship Contributions

Participated in research design: Liu, Tian, Zhang.
Conducted experiments: Liu, Li.
Performed data analysis: Liu, Xu, Song.
Wrote or contributed to the writing of the manuscript: Liu, Tian, Zhang.

References

Abe H, Odashima S, and Arichi S (1978a) The effects of saikosaponins on biological membranes. 2. Changes in electron spin resonance spectra from spin-labelled erythrocyte and erythrocyte ghost membranes. *Planta Med* **34**:287–290.

Abe H, Sakaguchi M, Konishi H, Tani T, and Arichi S (1978b) The effects of saikosaponins on biological membranes. 1. The relationship between the structures of saikosaponins and haemolytic activity. *Planta Med* **34**:160–166.

Abe H, Sakaguchi M, Yamada M, Arichi S, and Odashima S (1980) Pharmacological actions of saikosaponins isolated from Bupleurum falcatum. 1. Effects of saikosaponins on liver function. *Planta Med* **40**:366–372.

Abrahams HE and Robinson D (1969) β-D-Glucosidases and related enzymic activities in pig kidney. *Biochem J* **111**:749–755.

Ahn BZ and Sok DE (2006) Pharmacological activity of saikosaponins, in *Bupleurum Species: Scientific Evaluation and Clinical Applications* (Pan SL ed) pp 151–157, Taylor and Francis Group, Boca Raton, FL.

Ahn BZ, Yoon YD, Lee YH, Kim BH, and Sok DE (1998) Inhibitory effect of bupleuri radix saponins on adhesion of some solid tumor cells and relation to hemolytic action: screening of 232 herbal drugs for anti-cell adhesion. *Planta Med* **64**:220–224.

Bermejo Benito P, Abad Martínez MJ, Silván Sen AM, Sanz Gómez A, Fernández Matellano L, Sánchez Contreras S, and Díaz Lanza AM (1998) In vivo and in vitro antiinflammatory activity of saikosaponins. *Life Sci* **63**:1147–1156.

Brunton L, Parker K, Blumenthal D, and Buxton I (2008) *Goodman & Gilman's Manual of Pharmacology and Therapeutics*, 11th ed, McGraw-Hill, San Diego, CA.

Chen SM, Sato N, Yoshida M, Satoh N, and Ueda S (2008) Effects of Bupleurum scorzoneraefolium, Bupleurum falcatum, and saponins on nephrotoxic serum nephritis in mice. *J Ethnopharmacol* **116**:397–402.

Cheng PW, Ng LT, Chiang LC, and Lin CC (2006) Antiviral effects of saikosaponins on human coronavirus 229E in vitro. *Clin Exp Pharmacol Physiol* **33**:612–616.

Chiang LC, Ng LT, Liu LT, Shieh DE, and Lin CC (2003) Cytotoxicity and anti-hepatitis B virus activities of saikosaponins from Bupleurum species. *Planta Med* **69**:705–709.

Daniels LB, Coyle PJ, Chiao YB, Glew RH, and Labow RS (1981) Purification and characterization of a cytosolic broad specificity beta-glucosidase from human liver. *J Biol Chem* **256**: 13004–13013.

Fan J, Li X, Li P, Li N, Wang T, Shen H, Siow Y, Choy P, and Gong Y (2007) Saikosaponin-d attenuates the development of liver fibrosis by preventing hepatocyte injury. *Biochem Cell Biol* **85**:189–195.

Fujiwara K and Ogihara Y (1986) Pharmacological effects of oral saikosaponin a may differ depending on conditions of the gastrointestinal tract. *Life Sci* **39**:297–301.

Glew RH, Peters SP, and Christopher AR (1976) Isolation and characterization of beta-glucosidase from the cytosol of rat kidney cortex. *Biochim Biophys Acta* **422**:179–199.

Hattori T, Nishimura H, Kase Y, and Takeda S (2008) Saireito and saikosaponin D prevent urinary protein excretion via glucocorticoid receptor in adrenalectomized WKY rats with heterologous-phase anti-GBM nephritis. *Nephron Physiol* **109**:19–27.

Hsu MJ, Cheng JS, and Huang HC (2000) Effect of saikosaponin, a triterpene saponin, on apoptosis in lymphocytes: association with c-myc, p53, and bcl-2 mRNA. *Br J Pharmacol* **131**: 1285–1293.

Hsu YL, Kuo PL, and Lin CC (2004) The proliferative inhibition and apoptotic mechanism of Saikosaponin D in human non-small cell lung cancer A549 cells. *Life Sci* **75**: 1231–1242.

Huang HQ, Zhang X, Lin M, Shen YH, Yan SK, and Zhang WD (2008) Characterization and identification of saikosaponins in crude extracts from three Bupleurum species using LC-ESI-MS. *J Sep Sci* **31**:3190–3201.

Kaminsky LS and Zhang QY (2003) The small intestine as a xenobiotic-metabolizing organ. *Drug Metab Dispos* **31**:1520–1525.

Kida H, Akao T, Meselhy MR, and Hattori M (1998) Metabolism and pharmacokinetics of orally administered saikosaponin b1 in conventional, germ-free and Eubacterium sp. A-44-infected gnotobiote rats. *Biol Pharm Bull* **21**:588–593.

Kida H, Nakamura N, Meselhy MR, Akao T, and Hattori M (1997) Isolation and identification of human intestinal bacteria capable of hydrolyzing saikosaponins. *J Tradit Med* **14**:34–40.

Kim BM and Hong SH (2011) Sequential caspase-2 and caspase-8 activation is essential for saikosaponin a-induced apoptosis of human colon carcinoma cell lines. *Apoptosis* **16**: 184–197.

Kubota T and Hinoh H (1968) Triterpenoids from bupleurum falcatum L.—III: Isolation of genuine sapogenins, Saikogenins E, F and G. *Tetrahedron* **24**:675–686.

Kubota T, Tonami F, and Hinoh H (1966) The structure of saikogenins A, B, C and D, triterpenoid alcohols of bupleurum falcatum L. *Tetrahedron Lett* **7**:701–710.

Kumazawa Y, Kawakita T, Takimoto H, and Nomoto K (1990) Protective effect of saikosaponin A, saikosaponin D and saikogenin D against Pseudomonas aeruginosa infection in mice. *Int J Immunopharmacol* **12**:531–537.

Kumazawa Y, Takimoto H, Nishimura C, Kawakita T, and Nomoto K (1989) Activation of murine peritoneal macrophages by saikosaponin a, saikosaponin d and saikogenin d. *Int J Immunopharmacol* **11**:21–28.

Leung CY, Liu L, Wong RN, Zeng YY, Li M, and Zhou H (2005) Saikosaponin-d inhibits T cell activation through the modulation of PKCtheta, JNK, and NF-kappaB transcription factor. *Biochem Biophys Res Commun* 338:1920–1927.

Li P, Gong Y, Zu N, Li Y, Wang B, and Shimizu F (2005) Therapeutic mechanism of Saikosaponin-d in anti-Thy1 mAb 1-22-3-induced rat model of glomerulonephritis. *Nephron, Exp Nephrol* **101**:e111–e118.

Motoo Y and Sawabu N (1994) Antitumor effects of saikosaponins, baicalin and baicalein on human hepatoma cell lines. *Cancer Lett* **86**:91–95.

Nose M, Amagaya S, and Ogihara Y (1989a) Corticosterone secretion-inducing activity of saikosaponin metabolites formed in the alimentary tract. *Chem Pharm Bull (Tokyo)* **37**: 2736–2740.

Nose M, Amagaya S, and Ogihara Y (1989b) Effects of saikosaponin metabolites on the hemolysis of red blood cells and their adsorbability on the cell membrane. *Chem Pharm Bull (Tokyo)* **37**:3306–3310.

Robinson D (1956) The fluorimetric determination of beta-glucosidase: its occurrence in the tissues of animals, including insects. *Biochem J* **63**:39–44.

Segal R, Shud F, and Milo-Goldzweig I (1978) Hemolytic properties of synthetic glycosides. *J Pharm Sci* **67**:1589–1592.

Shimizu K, Amagaya S, and Ogihara Y (1984) Quantitative analysis of the metabolites of saikosaponin a using high-performance liquid chromatography. *J Chromatogr A* **307**:488–492.

Shimizu K, Amagaya S, and Ogihara Y (1985a) Structural transformation of saikosaponins by gastric juice and intestinal flora. *J Pharmacobiodyn* **8**:718–725.

Downloaded from dmd.aspetjournals.org at Zhejiang University on May 1, 2013

Shimizu K, Amagaya S, and Ogihara Y (1985b) New derivatives of saikosaponins. *Chem Pharm Bull (Tokyo)* **33**:3349–3355.
Sun Y, Cai TT, Zhou XB, and Xu Q (2009) Saikosaponin a inhibits the proliferation and activation of T cells through cell cycle arrest and induction of apoptosis. *Int Immunopharmacol* **9**:978–983.
Tang YH, Zhang YY, Zhu HY, and Huang CG (2007) A high-performance liquid chromatographic method for saikosaponin a quantification in rat plasma. *Biomed Chromatogr* **21**: 458–462.
Tsai YJ, Chen IL, Horng LY, and Wu RT (2002) Induction of differentiation in rat C6 glioma cells with Saikosaponins. *Phytother Res* **16**:117–121.
Wang P, Ren J, Tang J, Zhang D, Li B, and Li Y (2010b) Estrogen-like activities of saikosaponin-d in vitro: a pilot study. *Eur J Pharmacol* **626**:159–165.
Wang Q, Zheng XL, Yang L, Shi F, Gao LB, Zhong YJ, Sun H, He F, Lin Y, and Wang X (2010a) Reactive oxygen species-mediated apoptosis contributes to chemosensitization effect of saikosaponins on cisplatin-induced cytotoxicity in cancer cells. *J Exp Clin Cancer Res* **29**: 159–166.
Wen-Sheng W (2003) ERK signaling pathway is involved in p15INK4b/p16INK4a expression and HepG2 growth inhibition triggered by TPA and Saikosaponin a. *Oncogene* **22**: 955–963.
Wu SJ, Lin YH, Chu CC, Tsai YH, and Chao JC (2008) Curcumin or saikosaponin a improves hepatic antioxidant capacity and protects against CCl4-induced liver injury in rats. *J Med Food* **11**:224–229.
Xu L, Song R, Tian JX, Tian Y, Liu GQ, and Zhang ZJ (2012) Analysis of saikosaponins in rat plasma by anionic adducts-based liquid chromatography tandem mass spectrometry method. *Biomed Chromatogr* **26**:808–815.
Yokoyama H, Hiai S, and Oura H (1981) Chemical structures and corticosterone secretion-inducing activities of saikosaponins. *Chem Pharm Bull (Tokyo)* **29**:500–504.
Yu Y, Yang WX, Wang H, Zhang WZ, Liu BH, and Dong ZY (2002) Characteristics and mechanism of enzyme secretion and increase in [Ca2+]i in Saikosaponin(I) stimulated rat pancreatic acinar cells. *World J Gastroenterol* **8**:524–527.
Zhang H, Zhang D, Ray K, and Zhu M (2009) Mass defect filter technique and its applications to drug metabolite identification by high-resolution mass spectrometry. *J Mass Spectrom* **44**:999–1016.
Zhang QY, Kaminsky LS, Dunbar D, Zhang J, and Ding X (2007) Role of small intestinal cytochromes p450 in the bioavailability of oral nifedipine. *Drug Metab Dispos* **35**:1617–1623.
Zhu M, Ma L, Zhang D, Ray K, Zhao W, Humphreys WG, Skiles G, Sanders M, and Zhang H (2006) Detection and characterization of metabolites in biological matrices using mass defect filtering of liquid chromatography/high resolution mass spectrometry data. *Drug Metab Dispos* **34**:1722–1733.

Address correspondence to: Dr. Zunjian Zhang, Key Laboratory of Drug Quality Control and Pharmacovigilance, China Pharmaceutical University, 24 Tongjiaxiang, Nanjing 210009, China. E-mail: zunjianzhangcpu@hotmail.com

DMD
DRUG METABOLISM AND DISPOSITION
aspet
Downloaded from dmd.aspetjournals.org at Zhejiang University on May 1, 2013